

## Colloidal Stability of Magnetite/Poly(lactic acid) Core/Shell Nanoparticles

Salvador A. Gómez-Lopera,<sup>†</sup> José L. Arias,<sup>‡</sup> Visitación Gallardo,<sup>‡</sup> and Ángel V. Delgado<sup>\*,§</sup>

Department of Applied Physics, Polytechnic University of Cartagena, Spain,  
Department of Pharmacy and Pharmaceutical Technology, Faculty of Pharmacy, University of Granada,  
Spain, and Department of Applied Physics, Faculty of Sciences, University of Granada,  
18071 Granada, Spain

Received November 8, 2005. In Final Form: January 24, 2006

In this work, we describe an experimental investigation on the colloidal stability of suspensions of three kinds of particles, including magnetite, poly(lactic acid) (PLA), and composite core/shell colloids formed by a magnetite core surrounded by a PLA shell. The experiments were performed with dilute suspensions, so that recording the optical absorbance with time gives a suitable indication of the aggregation and sedimentation of the suspensions. The method allowed us to distinguish very accurately between the different surface and magnetic forces responsible for the structures acquired by particle aggregates. Thus, the pure PLA suspensions are very sensitive to ionic strength and almost unaffected by pH changes. On the contrary, the stability of magnetite systems is mainly controlled by pH. The effect of vertical magnetic fields on the stability of magnetite and magnetite/PLA suspensions is also investigated. The PLA shell reduces the magnetic responsiveness of magnetite, but it is demonstrated that the mixed particles can also form structures induced by the field, despite their lower magnetization, and they can be considered in magnetically targeted biomedical applications.

### Introduction

In a previous paper,<sup>1</sup> we described the preparation and characterization of a colloidal system with promising properties concerning its applications; this system consists of composite particles formed by a magnetic nucleus (magnetite) and a biodegradable polymer shell, poly(lactic acid) (PLA). We performed a systematic comparison between the electrokinetic, thermodynamic, and structural properties of the synthetic heterogeneous particles and those of their individual components, magnetite and PLA.

Suspensions of these particles could be ideal as drug vehicles, particularly in the treatment of solid tumors: their magnetic nucleus confers the particles' significant responsiveness to externally applied magnetic fields, which could be used to drive them to and keep them at the location of the body where the action of the chemotherapy agent might be needed. The drug can be loaded on the polymer shell, which, upon degradation in the body, would release the active principles.<sup>2–4</sup> A number of works have dealt with this kind of particle, consisting of a nucleus of iron oxide and a polymer shell or vice-versa.<sup>5–10</sup>

For such purposes, in addition to the control of the size, structure, and composition of the particles, it is essential to evaluate their colloidal stability. This is so because the presence of aggregates alters (decreases) the specific surface area of the system and, hence, its efficiency and usefulness as a drug vehicle. Also, it must be carefully considered that the drug-loaded particles must circulate through capillaries with diameters ranging down to 1.4  $\mu\text{m}$ , and should not grow to sizes large enough to obstruct them.

A wide variety of physical phenomenology was encountered, and hence the behavior of the individual components, magnetite and PLA, will first be discussed. Then these results will be considered together to explain the behavior of the composite particles.

This paper is organized as follows: After the description of the techniques for the preparation of the particles, we will present the methods of evaluation of their stability. Then we will show the effect of ionic strength and pH on the stability (indirectly deduced from the time evolution of the optical absorbance of the suspensions) of PLA, magnetite, and composite particles. Finally, attention will be given to the effect of the application of external magnetic fields of different strengths to the latter two kinds of suspensions.

### Materials and Methods

**Materials.** Magnetite spherical particles with an average diameter of  $160 \pm 60$  nm (Figure 1a is an example) were obtained according to the procedure of Sugimoto and Matijević,<sup>11</sup> with the following specific selection of the reactants concentrations and route of preparation:

1. Mix water (all water used in the experiments and in solutions preparation was ultrapurified in a Milli-Q Academic System, from Millipore, France), 5 M KOH (Merck, Germany), and 2 M KNO<sub>3</sub> (Merck, Germany) in the following respective amounts: 1050, 35, and 140 mL.

2. Dissolve 0.2 mL of H<sub>2</sub>SO<sub>4</sub> (diluted 1:1 with water; we used H<sub>2</sub>SO<sub>4</sub> puriss from Panreac, Spain), and 55.6 g of FeSO<sub>4</sub>·H<sub>2</sub>O

\* Corresponding author. Phone: +34-958-243-209. Fax: +34-958-243-214. E-mail: adelgado@ugr.es.

<sup>†</sup> Polytechnic University of Cartagena.

<sup>‡</sup> Department of Pharmacy and Pharmaceutical Technology, University of Granada.

<sup>§</sup> Department of Applied Physics, University of Granada.

(1) Gómez-Lopera, S. A.; Plaza, R. C.; Delgado, A. V. *J. Colloid Interface Sci.* **2001**, *240*, 40.

(2) Lübke, A. S.; Alexiou, C.; Bergemann, C. *J. Surg. Res.* **2001**, *95*, 200.

(3) Craig, D. Q. M. In *Technological Applications of Dispersions*; McKay, R. B., Ed.; Marcel Dekker: New York, 1994; Chapter 13.

(4) Goodwin, S.; Peterson, C.; Hoh, C.; Bittner, C. *J. Magn. Magn. Mater.* **1999**, *194*, 132.

(5) Pankhurst, Q. A.; Connolly, J.; Jones, S. K.; Dobson, J. *J. Phys. D: Appl. Phys.* **2003**, *36* (13), R167.

(6) Flesch, C.; Delaite, C.; Dumas, P.; Bourgeat-Lami, E.; Duguet, E. *J. Polym. Sci., Part A: Polym. Chem.* **2004**, *42* (23), 6011.

(7) Gupta, A. K.; Gupta, M. *Biomaterials* **2005**, *26* (18), 3995.

(8) Ren, J.; Hong, H. Y.; Ren, T. B. *Mater. Lett.* **2005**, *59* (21), 2655.

(9) Okassa, L. N.; Marchais, H.; Douziech-Eyrolles, L.; Cohen-Jonathan, S.; Souce, M.; Dubois, P.; Chourpa, I. *Int. J. Pharm.* **2005**, *302* (1–2), 187.

(10) Arias, J. L.; Gallardo, V.; Gómez-Lopera, S. A.; Plaza, R. C.; Delgado, A. V. *J. Controlled Release* **2001**, *77* (3), 309.

(11) Sugimoto, T.; Matijević, E. *J. Colloid Interface Sci.* **1980**, *74* (1), 227.

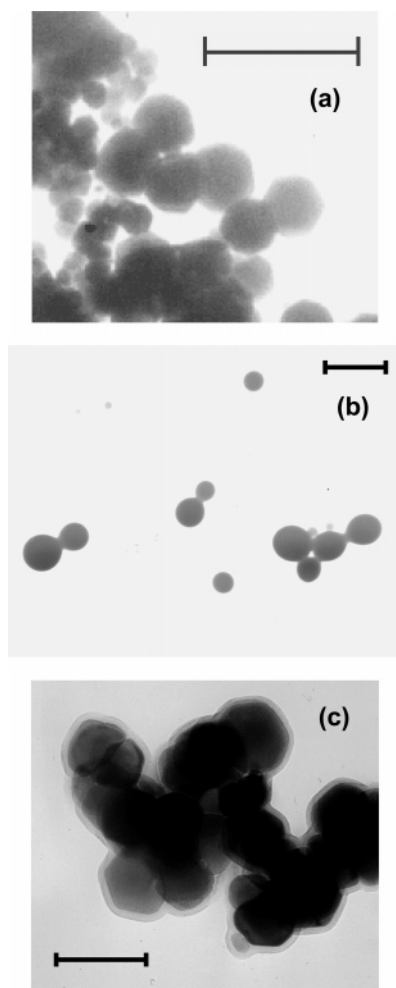


**Figure 1.** Transmission electron microscopy photographs of magnetite (a), PLA (b), and composite particles (c). Bar lengths: 500 nm (a), 4  $\mu\text{m}$  (b), and 200 nm (c).

(Panreac, Spain) in 200 mL of water previously purged with pure  $\text{N}_2$  for about 5 min.

3. Mix the two solutions thus prepared after bubbling them with  $\text{N}_2$  for 2 h.

4. Age the dark-green gel thus obtained for 4 h in a convection oven set at 90  $^\circ\text{C}$ .

5. Clean the obtained suspensions of both undesired ions and nonmagnetic particles by repeated sedimentation on a permanent magnet and redispersion in water. The magnetite particles must be kept dry if they will not be used shortly after their preparation, as they easily undergo oxidation to maghemite if kept in water.<sup>12</sup>

Concerning the preparation of PLA microspheres (average diameter  $1.7 \pm 0.5 \mu\text{m}$ ; Figure 1b), this is based on the methods previously described in the literature.<sup>13–21</sup> Specifically, we followed the steps detailed below, corresponding to the so-called double-emulsion method:

1. Dissolve 0.6 g of poly(DL-lactide) (Lactel BP-0500, Sigma-Aldrich, USA) in 40 mL of dichloromethane (Panreac, Spain).

2. Add 20 mL of water to the solution and homogenize at 14 000 rpm (Dixax 900 homogenizer, Heidolph, Germany) for a few seconds. The formation of a whitish dispersion (in fact, a water-in-oil (w/o) emulsion) is immediately observed.

3. Dissolve 2.5 g of poly(vinyl alcohol) (PVA;  $M_w$ : 89000–98000; Sigma-Aldrich, U.S.A.) in 250 mL of water previously heated to almost boiling. The solution is cooled in a refrigerator to reduce froth formation.

4. Add the w/o emulsion obtained in step 2 above to the PVA solution and homogenize again at 14 000 rpm. This will lead to the formation of a double emulsion that consists of droplets of the w/o emulsion dispersed in water [(water-in-oil)-in-water, or (w/o)/w, emulsion].

5. Evaporate the organic solvent remaining in the triple emulsion obtained in step 4 at room temperature under mild magnetic stirring of the double emulsion.

6. Clean the resulting suspension by serum replacement (UHP-76 filtration cell from MFS, Japan, with a 0.2  $\mu\text{m}$  pore diameter Millipore filter).

The procedure of preparation of magnetite/PLA core/shell particles with average diameter of  $180 \pm 50 \text{ nm}$  (see Figure 1c) was similar to that of bare PLA, except that, in the first w/o emulsion, we used a suspension of magnetite in water (particle concentration: 20% w/v) instead of just water. In addition, the magnetic responsiveness of the composites allowed us to use repeated magnetic separation (as with bare magnetite) to clean the suspensions of unreacted material.<sup>1</sup>

**Methods.** All our determinations of the stability of the suspensions were based on the measurement of their optical absorbance with a Dinko UV-Vis 8500 double-beam spectrophotometer (Dinko Instruments, Spain) set at a wavelength of 550 nm. Square glass cuvettes with a path length of 1 cm were used. Because of the very different densities of PLA and magnetite, their settling rates are correspondingly different, and hence we could not measure their stability in exactly the same fashion. Specifically, in the case of PLA, we could analyze both the increase in absorbance during the early steps of aggregation and its long-term decrease due to gravitational settling. In the case of magnetite and mixed particles, reliable information came mainly from experiments of the latter type.

Recall that for the materials and size ranges investigated, the application of scattering theories to the calculation of the extinction cross-section of a two-sphere aggregate yields a value larger than the sum of the cross-sections of the individual spheres.<sup>22–24</sup> This explains the expected increase in absorbance  $A$  at the earliest steps of aggregation, when dimer formation prevails. That increase will eventually be more than compensated for by the gravitational settling leading to a time decrease in  $A$ .

Let us finally mention that, to obtain the information concerning the early steps of aggregation, 3 mL of the suspension of PLA in water was placed in the cuvette in the spectrophotometer, and a small volume (0.15 mL) of a concentrated solution was rapidly added and mixed with a microsyringe, while  $A$  data were recorded. When long-time determinations were pursued, the suspension with previously added electrolyte was sonicated and placed in the spectrophotometer while absorbance was measured.

In the case of magnetite nuclei and core/shell particles, the determinations were always carried out using the latter method, but, because of the magnetic nature of these particles, it was essential to evaluate the effect of applied magnetic fields on the stability. This was carried out by placing the cuvette in the spectrophotometer in the center of a pair of horizontal Helmholtz coils 20 cm in radius (Phywe, Germany). A Hall-effect teslameter (also from Phywe) was used to measure the field strength.

(12) Plaza, R. C.; Arias, J. L.; Espín, M.; Jiménez, M. L.; Delgado, A. V. *J. Colloid Interface Sci.* **2002**, *245*, 86.

(13) Mauduit, J.; Bukh, N.; Vert, M. *J. Colloid Interface Sci.* **1993**, *23*, 209.

(14) Mauduit, J.; Bukh, N.; Vert, M. *J. Colloid Interface Sci.* **1993**, *23*, 221.

(15) Mauduit, J.; Bukh, N.; Vert, M. *J. Colloid Interface Sci.* **1993**, *25*, 43.

(16) Okada, H.; Yamamoto, M.; Heya, T.; Inoue, Y.; Kamei, S.; Ogawa, Y.; Toguchi, H. *J. Controlled Release* **1994**, *28*, 121.

(17) Aso, Y.; Yoshioka, S.; Po, A. L. W.; Terao, T. *J. Controlled Release* **1994**, *31*, 33.

(18) Llovet, M. I.; Egea, M. A.; Valero, J.; Alsina, M. A.; Garcia, M. L.; Chauvet, A. *Drug Dev. Ind. Pharm.* **1995**, *21*, 1761.

(19) Radwan, M. A. *Drug Dev. Ind. Pharm.* **1995**, *21* (20), 2371.

(20) Sah, H.; Chien, Y. W. *J. Pharm. Sci.* **1995**, *84*, 1353.

(21) Soriano, I.; Delgado, A.; Diaz, R. V.; Evora, C. *Drug Dev. Ind. Pharm.* **1995**, *21* (5), 549.

(22) Fuller, K. A. *J. Opt. Soc. Am. A* **1994**, *11*, 3251.

(23) Mackowski, D. W. *J. Opt. Soc. Am. A* **1994**, *11*, 2851.

(24) Plaza, R. C.; Quirantes, A.; Delgado, A. V. *J. Colloid Interface Sci.* **2002**, *252*, 102.

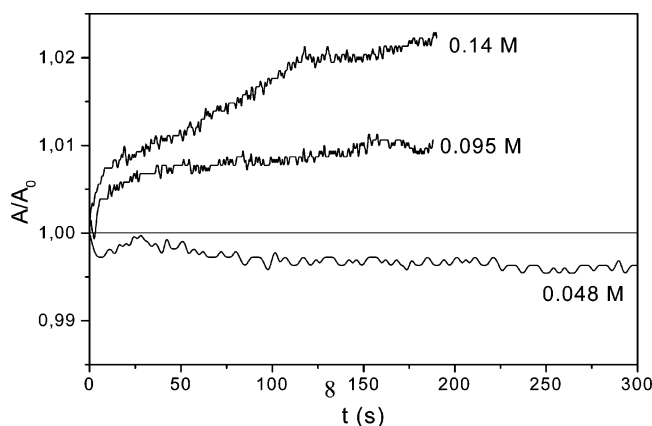


**Figure 2.** Time dependence of optical absorbance  $A$  (relative to its initial value,  $A_0$ ) of PLA suspensions after the rapid addition of NaCl solutions to yield the molar concentrations indicated. The concentration of solids was 0.06% (w/v). Natural pH = 5.5.

### Results and Discussion

**Absorbance Time for PLA Suspensions.** Figure 2 shows the evolution with time of the optical absorbance  $A$  (relative to its initial value,  $A_0$ ) of PLA suspensions during the first seconds after the addition of the indicated NaCl concentrations. Note how the sign of the initial slope of  $A/A_0-t$  curves changes from negative (weak aggregation, predominance of sedimentation) to positive (rapid coagulation), and then gets increasingly positive as the electrolyte concentration is increased.

The effect of electrolyte concentration on the stability can be more widely investigated using the second method described, that is, preparing the suspensions with the desired concentration and measuring the time dependence of  $A/A_0$  after redispersion by sonication. Figure 3a shows the results for PLA in NaCl solutions. The typical sigmoidal shape of the curves is clearly observed, and, in fact, they were fitted to the following general equation:

$$\frac{A}{A_0} = \frac{C_1 - C_2}{1 + e^{\frac{t - T_c}{\tau}}} + C_2 \quad (1)$$

where the characteristic times,  $T_c$  and  $\tau$ , are useful for quantitatively describing the settling behavior of the suspensions: if  $T_c$  is large, the suspensions take a long time to start settling, whereas, if  $\tau$  is large, the  $A/A_0$  fall is slow. In this and the following figures, the continuous lines always refer to the fitted curves. The fitting was performed using the nonlinear fit procedure included in the Origin 7.0 software package (OriginLab Corporation, Northampton, MA). Figure 3b shows the evolution of both times with the concentration of  $\text{KNO}_3$ . In this and similar plots, the error bars attached to the  $T_c$  and  $\tau$  data points correspond to the 95% confidence intervals for the fitted parameters. It is clearly observed that the polymer suspensions start settling earlier (lower  $T_c$ ) and settle at a faster rate (shorter  $\tau$ ) the larger the ionic strength. This is clear evidence of the instability induced by the addition of a sufficient concentration of ions, in accordance with the classical Derjaguin–Landau–Verwey–Overbeek (DLVO) theory.<sup>25</sup>

**Magnetite Suspensions.** Analysis of the colloidal stability of magnetite has the additional features associated to the effects of pH (because of the pH dependence of the surface charge of these particles) and magnetic fields. In addition, as Figure 4 shows, the response to ionic strength variations is also different in

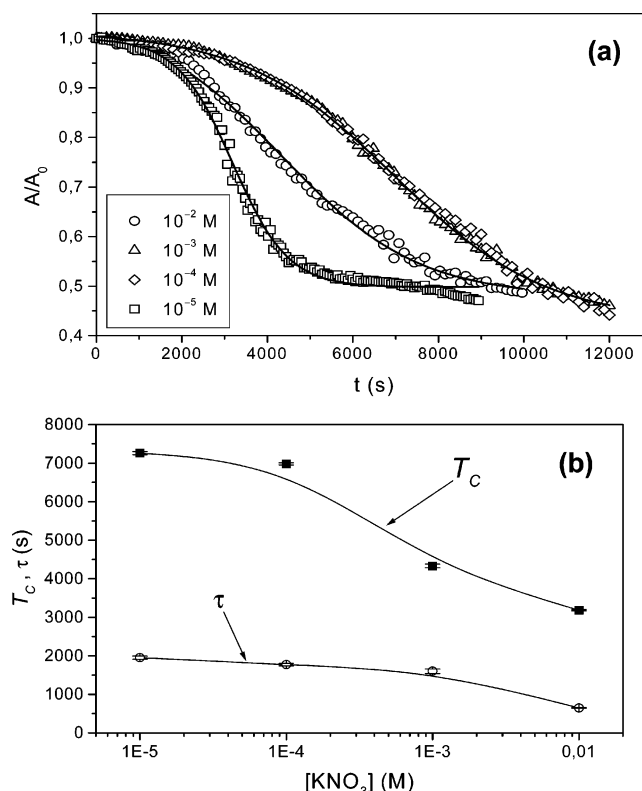


**Figure 3.** (a) Relative absorbance,  $A/A_0$ , of PLA suspensions (0.06% w/v concentration of solids) as a function of time for the  $\text{KNO}_3$  concentrations indicated. Natural pH = 5.5. (b) Characteristic times ( $T_c$ ,  $\tau$ ) (eq 1) of the curves in panel a, as a function of  $\text{KNO}_3$  concentration. The lines in panel a correspond to the fitted functions, while those in panel b are just a guide to the eye. The error bars in panel b correspond to 95% confidence intervals for the fitted parameters.

magnetite compared to PLA suspensions. We will focus on the variation of  $T_c$  and  $\tau$  with  $[\text{KNO}_3]$ : both parameters change with ionic strength in a similar way, as they increase when  $[\text{KNO}_3]$  is raised between  $10^{-5}$  and  $10^{-4}$  M, and then decrease and finally remain constant above 0.5 mM. The decline shown by both times above 0.1 mM is an indication of aggregation induced by ionic strength, and in fact, some sort of saturation (the critical coagulation concentration) is reached at about 0.5 mmol/L.

Much more significant is the effect of pH on the stability of magnetite suspensions, as Figure 5a,b demonstrates. The overall trends of the curves in Figure 5a, as well as the variation with pH of the times  $T_c$  and  $\tau$ , indicate a particular behavior in the vicinity of pH 7, which approximately corresponds to the isoelectric point or pH of the zero  $\zeta$  potential of magnetite.<sup>1,11</sup>  $\tau$  data indicate suspensions that settle very rapidly around that pH: once the magnetite suspensions start to settle down, they do it more rapidly the closer their pH is to the isoelectric condition. On the contrary,  $T_c$  is the largest in such conditions, and this can be explained by considering the fact that the electrostatic repulsion between particles is negligible at the isoelectric point: this would indeed favor particle–particle aggregation, and hence lead to faster sedimentation rate. However, the decrease in  $A/A_0$  brought about by the gravitational reduction in the turbidity of the suspensions is more than compensated by the increased extinction cross-section of the aggregates. For this reason,  $A/A_0$  takes a longer time to begin its reduction by settling, and  $T_c$  is highest at pH  $\sim 7$ .

A very noticeable feature of the curves in Figure 5a is the observed increased in  $A/A_0$  at a quite late stage of the sedimentation process; note the significant rise in absorbance found at pH 7

(25) Stechemesser, H.; Sonntag, H. In *Coagulation and Flocculation*; Stechemesser, H., Dobiás, B., Eds.; Taylor and Francis: Boca Raton, FL, 2004; Chapter 3.



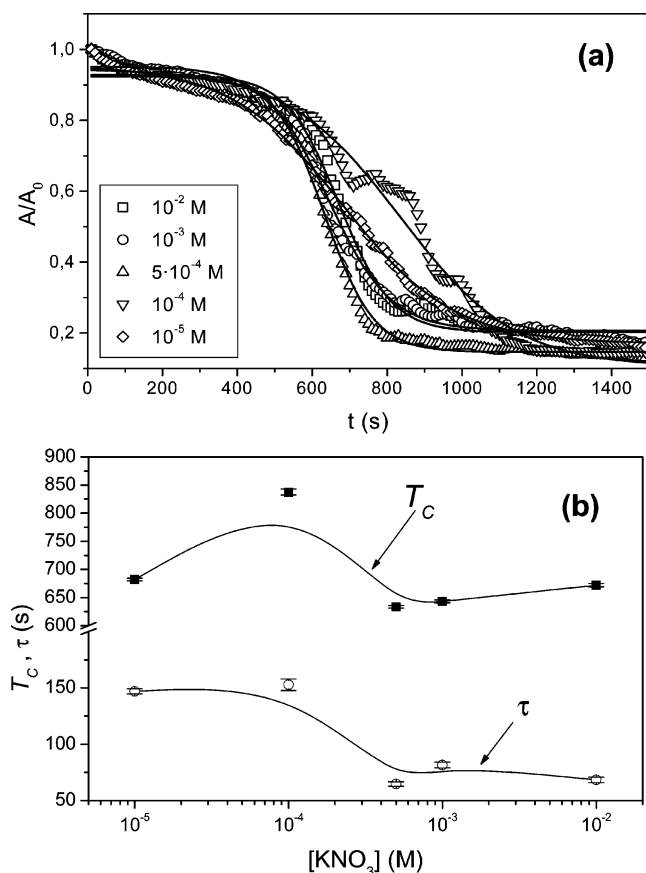


**Figure 4.** (a) Relative absorbance,  $A/A_0$ , of magnetite suspensions as a function of time for several  $\text{KNO}_3$  concentrations. Solid concentrations: 0.25 mg/mL. Natural pH = 5.5. (b) Characteristic times ( $T_c$ ,  $\tau$ ) (eq 1) of the  $A/A_0$ - $t$  dependences in panel a, as a function of  $\text{KNO}_3$  concentration. The lines in panel a correspond to the fitted functions, while those in panel b are just a guide to the eye. The error bars in panel b correspond to 95% confidence intervals.

and 9, and roughly occurring during the time interval extending between 500 and 900 s after the beginning of the experiment. We suggest that such maxima in  $A/A_0$  are a consequence of magnetic interactions between particles. Since these experiments were conducted in the absence of any applied magnetic field, attractions may exist because of the remnant magnetization of the particles previously subjected to the strong permanent magnet used for magnetic sedimentation. Taking into account that such a magnetization must be rather low, the effect of dipolar magnetic attraction will be observable only if it is not surpassed by electrostatic repulsion. For this reason, the maximum in  $A/A_0$  does not occur when the pH is  $< 5.1$  or  $> 9$ , that is, when the surface charge is higher, either positive or negative. In addition, that must also be the reason the process is so slow and takes several minutes to be noticed. Less intuitive is the fact that the maximum is more intense and occurs earlier at pH = 9 and at pH = 7, the isoelectric point. It can be proposed that the universal, isotropic, van der Waals attraction (the only nonmagnetic one occurring at  $\text{pH}_{\text{iep}}$ ) gives little chance for magnetic attractions to manifest. The mild electrostatic repulsion at pH = 9 must partly neutralize the van der Waals attraction and give way to the magnetic dipolar attraction.

**Effect of External Magnetic Fields.** The weak magnetic attraction mentioned above can be magnified by application of an external field, which will induce significantly larger magnetization. As we will see below, the application of vertical magnetic fields increases  $T_c$  and  $\tau$ , and makes the maxima in the  $A/A_0$ - $t$  curves that we have found before much more appreciable.

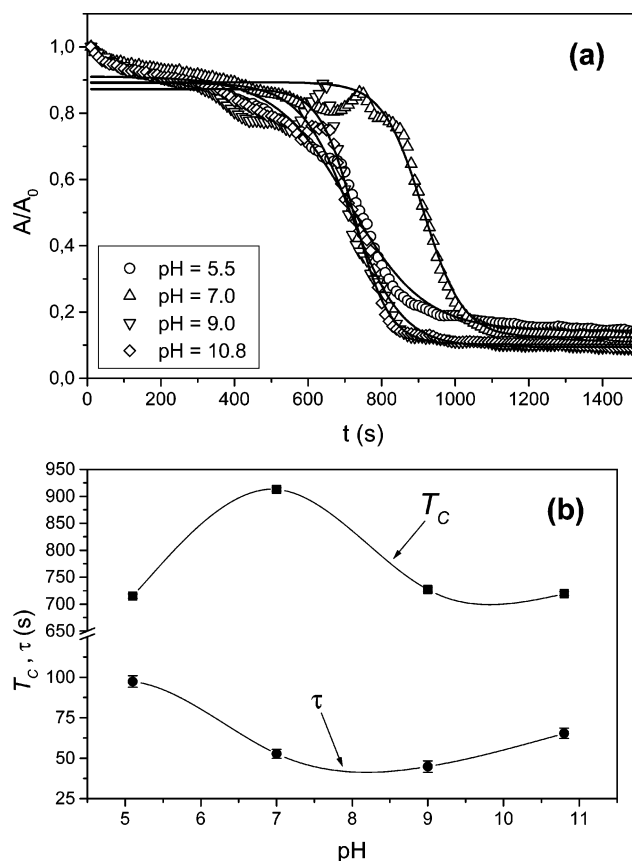


**Figure 5.** (a) Relative absorbance,  $A/A_0$ , of magnetite suspensions as a function of time for several pH values. Ionic strength: 1 mmol/L  $\text{KNO}_3$ ; solid concentration: 0.25 mg/mL. (b) Characteristic times ( $T_c$ ,  $\tau$ ) (eq 1) of the time evolution of  $A/A_0$  in panel a, as a function of pH. The lines in panel a correspond to the fitted functions, while those in panel b are just a guide to the eye. The error bars in panel b correspond to 95% confidence intervals.

Figure 6a (compare it to Figure 5a) shows  $A/A_0$ - $t$  data as a function of pH in the presence of a 2.5 mT magnetic induction  $B$ , directed vertically upward. The comparison with the zero-field condition can be made quantitatively with reference to Figure 6b, which generally confirms our previous arguments: the action of the field induces the formation of chains of particles oriented parallel to the field and is affected little by gravity. This is a well-known effect, responsible for the enhancement of viscosity and yield stress (magnetorheological effect) in suspensions of magnetic particles.<sup>26-29</sup>

The presence of such structures explains the larger  $T_c$  values. They will eventually break down (in fact, the field strength is not very high), and  $A/A_0$  will begin to decrease, but that rupture is not very easy, and  $\tau$  values are also longer in the presence of the field.

Perhaps, the most striking feature of the action of the field is the above-mentioned effect on the long-time maxima in  $A/A_0$  and on the time in which such maxima appear. It is precisely at the instant in which they appear, and on their duration, that the action of the field is more manifestly clear: both the time and duration increase upon application of  $B$ , suggesting that the building of the magnetic structure is a large-scale phenomenon that dominates over other aspects of the sedimentation curve.

(26) Ginder, J. M. *MRS Bull.* **1998**, 23, 26.

(27) Phulé, P. P.; Ginder, J. M. *MRS Bull.* **1998**, 23, 19.

(28) De Vicente, J.; López-López, M. T.; González-Caballero, F.; Durán, J. D. G. *J. Rheol.* **2003**, 47, 1093.

(29) De Vicente, J.; López-López, M. T.; Durán, J. D. G.; Bossis, G. *J. Colloid Interface Sci.* **2005**, 282, 193.

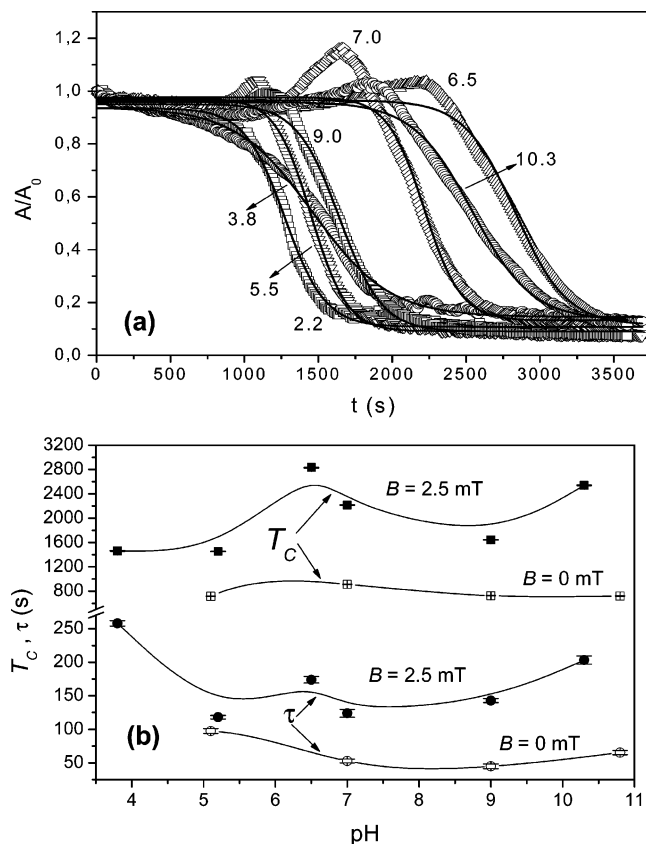


**Figure 6.** (a) Relative absorbance,  $A/A_0$ , of magnetite suspensions as a function of time for the indicated pH values, in the presence of a 2.5 mT vertical magnetic induction  $B$ . Ionic strength: 1 mmol/L  $\text{KNO}_3$ ; solid concentration: 0.25 mg/mL. (b) Characteristic times ( $T_c$ ,  $\tau$ ) (eq 1) of the time evolution of  $A/A_0$  in panel a, as a function of pH, in the presence of a 2.5 mT vertical magnetic induction  $B$ . The values corresponding to  $B = 0$  mT are included for comparison. The lines in panel a correspond to the fitted functions, while those in panel b are just a guide to the eye. The error bars in panel b correspond to 95% confidence intervals.

The height of the maxima (compare Figures 5a and 6a) does not change significantly from  $B = 0$  to  $B = 2.5$  mT. This can be understood by considering the fact that, once a given point is reached in the process of aggregation, the size of the aggregates is so large that from that moment on, the decrease in  $A/A_0$  due to sedimentation dominates the process, whether the field is applied or not.

The results in Figures 5 and 6 show that, except for the differences described, the variation of  $A/A_0$  with pH is comparable with and without field. The same can be said concerning the effect of electrolyte concentration; we show only the variation of  $T_c$  and  $\tau$  with  $[\text{KNO}_3]$ , instead of the full absorbance curves, in Figure 7.

Let us finally consider the influence of variations in the field strength and direction. Figure 8 shows some results. The shape of the curves in Figure 8a is the expected one: good separation from the  $B = 0$  case, greater effect with a larger field, and nonsignificant differences between the field-up and field-down situations. The latter aspects are clearly observable in Figure 8b, which includes the dependence of  $T_c$  and  $\tau$  on the field strength and direction.

**Effect of the Polymer Shell: Stability of Composite Particles.** Let us now consider how the responses of the stability to magnetic field, ionic strength, or pH of magnetite and PLA combine to give the stability of mixed magnetite/polymer particles. Because of the magnetic nucleus, we expect some sort

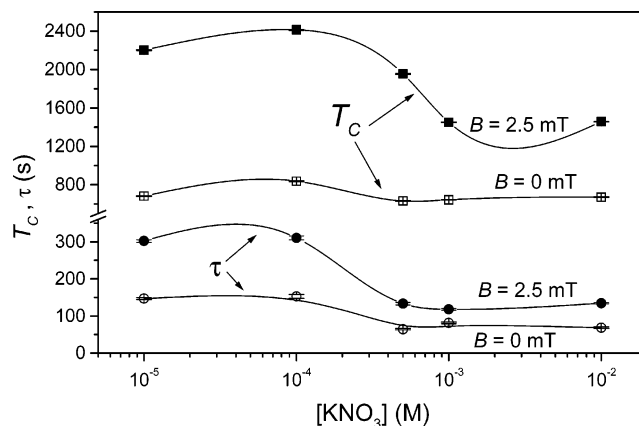


**Figure 7.** Characteristic times ( $T_c$ ,  $\tau$ ) (eq 1) of  $A/A_0$ - $t$  curves as a function of the concentration of  $\text{KNO}_3$  for magnetite suspensions in the presence and in the absence of a 2.5 mT vertical magnetic induction  $B$ . Solid concentration: 0.25 mg/mL. Natural pH = 5.5. The lines are just a guide to the eye. The error bars correspond to 95% confidence intervals.

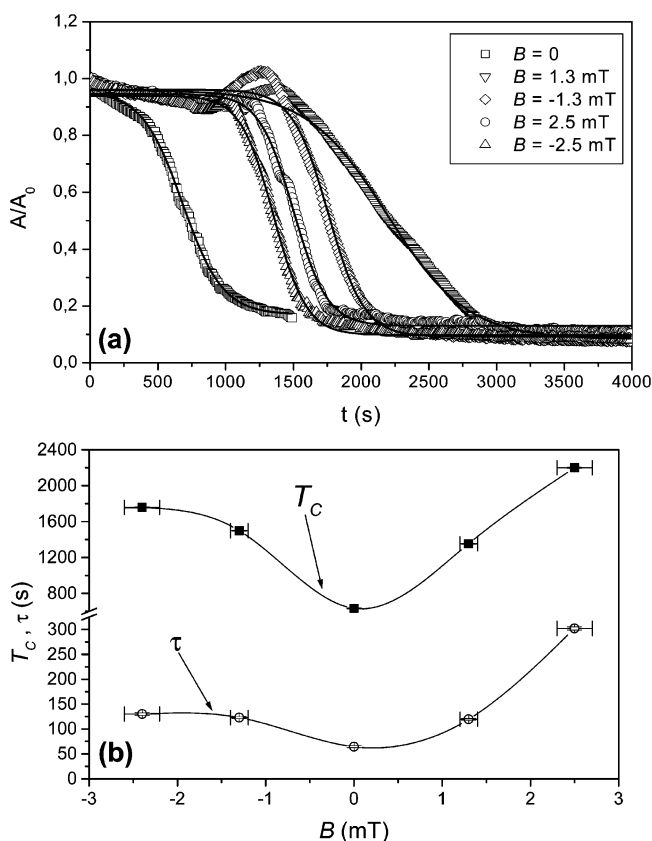


**Figure 8.** (a) Relative absorbance,  $A/A_0$ , as a function of time for magnetite suspensions containing 0.25 mg/mL of solids in  $10^{-5}$  mol/L  $\text{KNO}_3$  solution for the  $B$  values indicated. (b) The corresponding characteristic times ( $T_c$ ,  $\tau$ ) (eq 1). Positive (negative) fields correspond to the upward (downward) direction. The lines in panel a correspond to the fitted functions, while those in panel b are just a guide to the eye. The error bars in panel b correspond to 95% confidence intervals.

of effect of externally applied magnetic fields, whereas the PLA shell should hide the pH effect on the sedimentation rate of bare magnetite particles.

Figure 9 shows  $A/A_0$  as a function of time for 0.75 g/L suspensions of mixed particles in different  $\text{KNO}_3$  solutions, both in the presence and absence of a vertical magnetic induction  $B = 2.5$  mT. As observed, the curves display an exponential decrease, rather than a sigmoidal trend. In fact, we found that

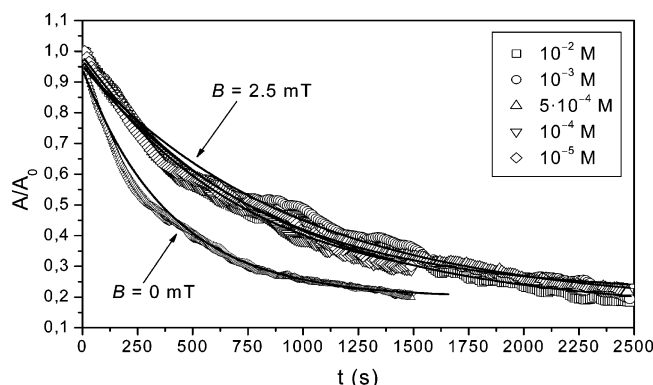


**Figure 9.** Relative absorbance,  $A/A_0$ , of magnetite/PLA particles plotted as a function of time for several  $\text{KNO}_3$  concentrations, with and without a 2.5 mT vertical magnetic induction  $B$ . The particle concentration was 0.75 g/L in all cases. Natural pH = 5.5. The lines correspond to the fitted functions.

the data could be well described by an equation of the following type:

$$\frac{A}{A_0} = C_3 + C_4 \exp(-t/\tau) \quad (2)$$

where  $\tau$  is a relaxation time. At short times ( $t \ll \tau$ ),  $A/A_0$  will depend linearly on  $t$ , with a slope

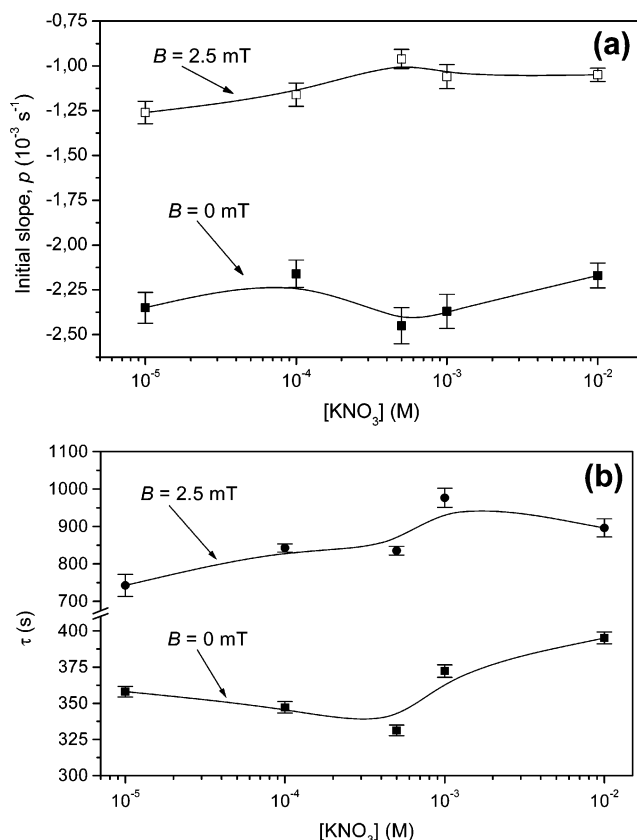
$$p = \left. \frac{d(A/A_0)}{dt} \right|_{t/\tau} = -\frac{C_4}{\tau} \quad (3)$$

Figure 10 shows the values of  $p$  and  $\tau$  deduced from the data in Figure 9 as a function of the concentration of  $\text{KNO}_3$ , with and without field applied. The data show, first of all, that we can use magnetic fields to control the stability of the composite colloids: the smaller  $|p|$  values, as well as the larger relaxation times,  $\tau$ , obtained in the presence of the field are indicative of systems that sediment slowly, which can be explained by the field-induced structure acquired by the suspensions. However, the effect of ionic strength is not significant, and only a slight increase in  $\tau$  with  $[\text{KNO}_3]$  can be observed. It must be taken into account that the effects of aggregation on the extinction cross-section of aggregates of core/shell particles is not known with precision.

Concerning the effect of pH on the stability, Figure 11 demonstrates that its noticeable influence in the case of magnetite (Figure 5) is almost completely lost, and we can only say that the field again induces a structure, which makes the overall  $A/A_0$  trends slower than in its absence.

### Conclusions

In this work we have shown that determinations of the optical absorbance of the suspensions as a function of time can help in the evaluation of the stability of systems consisting of particles formed by a magnetite nucleus and a PLA shell. In addition, the differences between the stability of the mixed particles and that of the bare components has also been demonstrated. Thus, the pH sensitivity of the stability of magnetite particles is hidden by the polymer shell, whose charge is essentially pH-independent. The interesting feature that external magnetic fields induce a



**Figure 10.** Initial slope  $p$  (a) and relaxation time  $\tau$  (b) of the data in Figure 9, after fitting them to eq 2. The lines are just a guide to the eye. The error bars correspond to 95% confidence intervals.

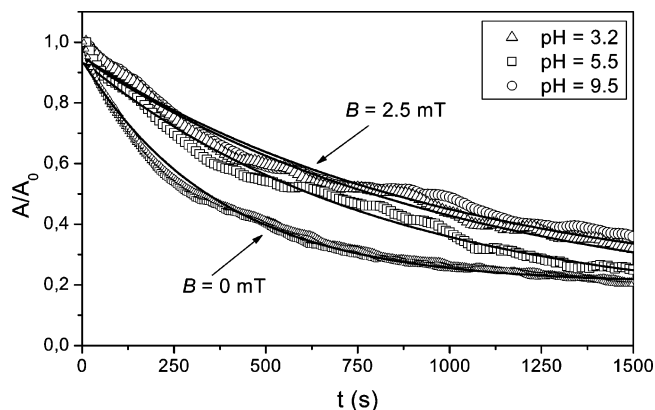


**Figure 11.** Relative absorbance,  $A/A_0$ , of magnetite/PLA particles plotted as a function of time for different pH values, with and without a 2.5 mT vertical magnetic induction  $B$ . Ionic strength:  $10^{-3}$  mol/L  $\text{KNO}_3$ ; solid concentration: 0.75 g/L. The lines correspond to the fitted functions.

structure in the suspensions of composite particles and permit control of their stability has also been clearly found with the techniques used.

**Acknowledgment.** Financial support from CICYT, Spain, under Projects MAT2004-00866 and MAT2005-07746-CO2, and from FEDER Funds (EU), are gratefully acknowledged.

LA0530079